Published in final edited form as:
Nat Med. ; 17(11): 1498–1503. doi:10.1038/nm.2492.

Adipocytes promote ovarian cancer metastasis and provide energy for rapid tumor growth

Kristin M Nieman[1], **Hilary A Kenny**[1], **Carla V Penicka**[1], **Andras Ladanyi**[1], **Rebecca Buell-Gutbrod**[2], **Marion R Zillhardt**[1], **Iris L Romero**[1], **Mark S Carey**[3], **Gordon B Mills**[3], **Gökhan S Hotamisligil**[4], **S Diane Yamada**[1], **Marcus E Peter**[5], **Katja Gwin**[2], and **Ernst Lengyel**[1]

[1]Department of Obstetrics and Gynecology/Section of Gynecologic Oncology, Center for Integrative Science, Chicago, Illinois, USA.

[2]Department of Pathology, University of Chicago, Chicago, Illinois, USA.

[3]Department of Systems Biology, MD Anderson Cancer Center, Houston, Texas, USA.

[4]Department of Genetics and Complex Diseases and the Broad Institute of Harvard University and Massachusetts Institute of Technology, Harvard School of Public Health, Boston, Massachusetts, USA.

[5]Feinberg School of Medicine, Division of Hematology and Oncology, Northwestern University, Chicago, Illinois, USA.

Abstract

Intra-abdominal tumors, such as ovarian cancer[1,2], have a clear predilection for metastasis to the omentum, an organ primarily composed of adipocytes. Currently, it is unclear why tumor cells preferentially home to and proliferate in the omentum, yet omental metastases typically represent the largest tumor in the abdominal cavities of women with ovarian cancer. We show here that primary human omental adipocytes promote homing, migration and invasion of ovarian cancer cells, and that adipokines including interleukin-8 (IL-8) mediate these activities. Adipocyte–ovarian cancer cell coculture led to the direct transfer of lipids from adipocytes to ovarian cancer cells and promoted *in vitro* and *in vivo* tumor growth. Furthermore, coculture induced lipolysis in adipocytes and β-oxidation in cancer cells, suggesting adipocytes act as an energy source for the cancer cells. A protein array identified upregulation of fatty acid–binding protein 4 (FABP4, also

Correspondence should be addressed to E.L. (elengyel@uchicago.edu)..

AUTHoR CONTRIBUTIONS

K.M.N. and H.A.K. performed most of the experiments. C.V.P. performed the western blots. M.R.Z., I.L.R. and C.V.P. assisted with some of the animal experiments. A.L., M.S.C. and G.B.M. performed and interpreted the protein array experiments. R.B.-G. and K.G. contributed to the immunohistochemistry for the human and mouse experiments. S.D.Y. and E.L. collected ovarian cancer tissues and clinicopathologic patient information. G.S.H. provided the *Fabp4*$^{-/-}$ mice and edited the manuscript. M.E.P. performed the bioinformatics analysis and edited the manuscript. K.M.N., H.A.K. and E.L. designed the experiments. K.M.N. and E.L. wrote the manuscript. E.L. directed the study.

Supplementary information is available on the Nature Medicine website.

COMPETING FINANCIAL INTERESTS

The authors declare competing financial interests: details accompany the full-text HTML version of the paper at http://www.nature.com/naturemedicine/.

Additional methods. Detailed methodology is described in the **Supplementary Methods**.

known as aP2) in omental metastases as compared to primary ovarian tumors, and FABP4 expression was detected in ovarian cancer cells at the adipocyte-tumor cell interface. FABP4 deficiency substantially impaired metastatic tumor growth in mice, indicating that FABP4 has a key role in ovarian cancer metastasis. These data indicate adipocytes provide fatty acids for rapid tumor growth, identifying lipid metabolism and transport as new targets for the treatment of cancers where adipocytes are a major component of the microenvironment.

Most ovarian cancers are diagnosed at an advanced stage when the tumor is widely metastatic[1,2]. The most common subtype is serous ovarian cancer, which may arise from the surface of the ovary or, as recently suggested, the fimbriated end of the fallopian tube[3]. The main site of ovarian cancer metastasis is the omentum, and 80% of all women with serous ovarian carcinoma present with omental meta-stases. The omentum, a large (20 × 12 × 3 cm) fat pad that extends from the stomach and covers the bowel (**Supplementary Fig. 1a**), functions as an endocrine organ and storage site for energy-dense lipids[4]. Ovarian cancer metastasis to the omentum results in transformation of this soft pad of tissue, primarily composed of adipocytes, to a solid tumor histologically devoid of adipocytes (**Supplementary Fig. 1b Fig. 1a**). If metastasis was a random event, all organs in contact with peritoneal fluid would have an equal distribution of metastases. However, both primary and recurrent high-grade serous ovarian carcinomas preferentially metastasize to adipose tissue. The molecular mechanisms underlying this predilection are unknown. Recognizing the importance of the microenvironment, we considered the possibility that adipocytes contribute to the metastatic cascade.

Ovarian cancer metastasis can be mimicked in female athymic nude mice by injecting fluorescently-labeled SKOV3ip1 human ovarian cancer cells intraperitoneally. After 20 min, a majority of tumor cells homed to the omentum (**Fig. 1b**). Because most cells in the omentum are adipocytes, we determined whether purified, viable adipocytes[5] from normal human omentum (**Supplementary Fig. 2a**) promoted the early steps of ovarian cancer metastasis, migration and invasion. SKOV3ip1 human ovarian cancer cells were placed in the top compartment of a Boyden chamber and adipocytes or conditioned medium from adipocytes in the bottom. Human omental adipocytes induced migration of SKOV3ip1 cells. Because the addition of omental adipocyte-conditioned medium had a greater effect on migration than the addition of omen-tal adipocytes, we suspected this effect was mediated by soluble factors (**Fig. 1c**). Invasion was more potently stimulated by omental adipocytes than adipocyte-contained medium (**Fig. 1d**). Comparing omental with subcutaneous adipocytes, we found that omental adipocytes were significantly more efficient in promoting invasion of ovarian cancer cells (**Fig. 1e**). In addition, invasion was promoted by omental adipocytes in gastric, breast and colon cancer cells (**Supplementary Fig. 2b**). In contrast, neither nontransformed human ovarian surface epithelial cells nor primary omental fibroblasts invaded in the presence of adipocytes.

To identify factors responsible for attracting ovarian cancer cells to the omentum, we performed a cytokine array (**Fig. 1f**). Among 62 cytokines tested, the five cytokines most abundantly secreted by omental adipocytes were IL-6, IL-8, monocyte chemoattractant protein-1 (MCP-1), tissue inhibitor of metalloproteinases-1 (TIMP-1) and adiponectin.

Antibody-mediated inhibition of IL-6, IL-8, MCP-1 and TIMP-1 resulted in a reduction of *in vitro* ovarian cancer cell homing toward adipocytes by at least 50% (**Fig. 1g**). Inhibition of IL-6 and IL-8 receptors (IL-6R and IL-8R), as well as their ligands, IL-6 and IL-8, using neutralizing antibodies[6,7] reduced adhesion of SKOV3ip1 cells to sections of human omentum and migration toward primary human omental adipocytes *in vitro* (**Fig. 1h** and **Supplementary Fig. 3a**). A neutralizing antibody against the IL-8R (CXCR1) reduced *in vivo* homing of ovarian cancer cells to the mouse omentum more efficiently than the IL-6R–specific inhibitory antibody (**Supplementary Fig. 3b**). Notably, CXCR1 expression was strongly upregulated in ovarian cancer cells, whereas the expression of IL-6R or its accessory protein, glycoprotein 130 (gp130), remained unchanged after cocultivation with adipocytes **(Supplementary Fig. 3c,d)**. Congruently, mitogenic signaling was induced in ovarian cancer cell adipocytes (ref. 6) through p38 mitogen-activated protein kinase and signal transducer and activator of transcription 3 phosphorylation (**Fig. 1i**). Activation of p38 was partially reversed by a CXCR1-neutralizing antibody (**Supplementary Fig. 3e**). These data indicated that adipocytes promote the early steps of ovarian cancer metastasis to the omentum, although a mechanistic explanation for the prevalence of omental metastatic tumors in women with ovarian cancer remained elusive.

Adipocytes promote the growth of cancer cells[8–10]. Because adipocytes comprise a majority of the omentum and store triglycerides, we hypothesized that adipocytes provide energy-dense lipids to ovarian cancer cells to support rapid growth. Remarkably, in tissue from women with omental metastasis, the ovarian cancer cells at the adipocyte–cancer cell interface contained abundant lipids (**Fig. 2a** and **Supplementary Fig. 4**). Notably, coculture of ovarian, breast or colon cancer cells with adipocytes resulted in cytoplasmic lipid droplet accumulation in the cancer cells (**Fig. 2b** and **Supplementary Fig. 5a**), which we confirmed by transmission electron microscopy (**Fig. 2c**). Coculture with omental or peritoneal adipocytes led to the greatest lipid accumulation in ovarian cancer cells compared to cocultures with subcutaneous or bowel mesenteric adipocytes (**Supplementary Fig. 5b**).

To determine whether the lipids detected in cancer cells after coculture were derived from adipocytes and not *de novo* lipogenesis, we cultured cancer cells with adipocytes that had been loaded with fluorescently labeled lipids. During coculture, fluorescent lipids were transferred from adipocytes to SKOV3ip1 cells (**Fig. 2d**), supporting a model in which adipocytes provide lipids to support tumor growth. Consistent with these results, the coculture of three different ovarian cancer cell lines, including the recently established primary ovarian cancer cell line, MONTY-1 (ref. 11), with adipocytes led to a significant increase in cancer cell proliferation *in vitro* (**Fig. 2e** and **Supplementary Fig. 5c**). *In vivo*, subcutaneous injection of SKOV3ip1 cells with primary human omental adipocytes into the flanks of nude mice produced tumors that were, on average, three times larger than tumors produced by SKOV3ip1 cells alone[12] (**Fig. 2f**).

Our results indicated that adipocytes provide a proliferative advantage and transfer fatty acids to ovarian cancer cells (**Fig. 2**). Thus, we suspected that the interaction between adipocytes and ovarian cancer cells results in metabolic alterations in both cell types. The interaction between adipose tissue and contracting muscle supplies an analogous physiological model for the interaction between ovarian cancer cells and adipocytes. The

energy for contracting muscle is provided by fatty acids mobilized from adipocytes[13]. The transport of free fatty acids depends on the lipolysis of stored triglycerides to free fatty acids and glycerol. Lipolytic activation in adipocytes commonly results from β-adrenergic receptor stimulation[14]. Subsequently, receptor activation elicits a G protein–coupled cascade and ultimately phosphorylation of hormone-sensitive lipase (HSL) and perilipin A, the rate-limiting enzymes in triglyceride hydrolysis[15] and the lipid droplet gate-keeper[16], respectively. To understand the effect ovarian cancer cells have on adipocytes, we assessed adipocyte metabolism. In the presence of ovarian cancer cells, adipocytes released significantly more free fatty acids and glycerol[17] than adipocytes cultured alone (**Fig. 3a,b**). Perilipin mRNA levels (**Supplementary Fig. 6a**) and HSL phosphorylation (**Fig. 3c,d**) were also induced in primary human omental adipocytes. Furthermore, propranolol, the β-adrenergic receptor antagonist, partially reversed ovarian cancer cell–induced HSL activation (**Supplementary Fig. 6b**). Taken together, these findings suggest cancer cells induce adipocyte lipolysis.

Next, we evaluated metabolic alterations in ovarian cancer cells after coculture with adipocytes. AMP-activated protein kinase (AMPK) is a central metabolic sensor that, upon phosphorylation, favors energy producing processes by inhibiting lipogenesis and activating β-oxidation[18]. This metabolic switch is regulated by the phosphorylation of acetyl-CoA carboxylase (ACC). Phosphorylation of ACC by AMPK or, to a lesser extent, protein kinase A[19] results in its inactivation and inability to inhibit carnitine palmitoyltransferase 1 (CPT1). CPT1 is the rate-limiting enzyme regulating mitochondrial import of fatty acids for β-oxidation in the form of acyl-CoA. Coculture of SKOV3ip1 cells with human omental adipocytes increased the phosphorylation of AMPK (**Fig. 3e,f**), the activity of protein kinase A (**Supplementary Fig. 6c**) and the rate of β-oxidation (**Fig. 3g** and **Supplementary Fig. 6d**) in ovarian cancer cells. This was paralleled by an increase in mRNA levels of CPT1 and acyl-CoA oxidase 1, the first enzyme in the β-oxidation pathway (**Fig. 3h**). These data suggest that adaptation of lipid metabolism allows ovarian cancer cells to thrive on lipids acquired from adipocytes.

In an effort to understand molecular differences induced by omental adipocytes, we compared primary ovarian cancer tissue and omental metastatic tissue from 22 women with advanced serous carcinoma using a reverse-phase protein array[20]. Of note, seven of the ten most upregulated or activated proteins in the omental metastases (**Supplementary Fig. 7a**) were known regulators of cancer cell growth (retinoblastoma protein, mammalian target of rapamycin and signal transducer and activator of transcription 5) and metabolism (phosphoinositide 3-kinase, total and phosphorylated ACC, and FABP4). The array showed that total and phosphorylated ACC amounts were significantly higher in omental metastases as compared to the primary tumor, which is consistent with an inhibition of lipogenesis in a lipid-rich omental environment (**Supplementary Fig. 7a–c**).

The protein with the third largest change in expression between primary tumors and metastases was FABP4. FABP4 reversibly binds long-chain fatty acids and is highly expressed in adipocytes[21,22]. In primary ovarian tumors, FABP4 expression was low; however, we found upregulation of FABP4 expression in all omental metastases, which we validated by immunoblotting (**Supplementary Fig. 7a,d,e**). Immunohistochemical staining

comparing primary ovarian tumor and corresponding omental metastatic tissues in twenty additional pairs revealed that FABP4 was strongly expressed in ovarian cancer cells at the adipocyte-cancer cell interface (**Fig. 4a**). In contrast, we did not detect FABP4 staining in ovarian cancer cells distant from the adipocyte-cancer cell interface in omental metastatatic tissue, in tissue from the corresponding primary ovarian tumor or in the adjacent benign ovarian stroma (**Fig. 4a**). The upregulation of FABP4 in metastatic human ovarian cancer samples could be mimicked *in vitro*; cocultivation of several cancer cell lines (ovarian, breast and colon) with adipocytes induced FABP4 mRNA expression, suggesting this induction is not limited to ovarian cancer cells (**Supplementary Fig. 8a**).

FABP4 staining of normal tissue from human organs showed FABP4 was expressed in endothelial cells and adipocytes from different anatomic locations (subcutaneous, peritoneal, mesenteric, omental and cancer-associated omental tissues) independent of the tissue origin (**Supplementary Fig. 8b–d**). FABP4 has been shown to regulate lipolysis[23], and its actions can be blocked by small-molecule inhibitors[24]. When we added a FABP4 inhibitor[25] to the coculture of ovarian cancer cells and adipocytes, lipid accumulation in the cancer cells (**Fig. 4b**) and adipocyte-mediated invasion (**Fig. 4c**) were drastically reduced. However, using the inhibitor did not clarify whether FABP4 expression in adipocytes or cancer cells is important for its tumor-promoting functions. Therefore, ovarian cancer tumor growth in aP2-knockout (*Fabp4*$^{-/-}$) mice was assessed. *Fabp4*$^{-/-}$ mice have reduced insulin resistance following environmentally[21] or genetically[26] induced obesity; however, the effect of FABP4 deficiency on cancer growth or metastasis has not been determined. After we confirmed the absence or presence of FABP4 mRNA and protein expression in adipose tissue from *Fabp4*$^{-/-}$ and wild-type (WT) mice (**Supplementary Fig. 9a–c**), we injected ID8 mouse ovarian cancer cells either intraperitoneally or orthotopically under the ovarian bursa. In the intraperitoneal model, we observed a significant reduction in tumor burden in the absence of FABP4 (**Fig. 4d**). This was paralleled by a reduction in microvessel density (CD31) and tumor cell proliferation (Ki-67), with no change in caspase-3 activation in tumors from *Fabp4*$^{-/-}$ mice (**Supplementary Fig. 9d**), suggesting host FABP4 is important for tumor cell growth without affecting apoptosis. Notably, in the more relevant orthotopic model, when ovarian cancer cells are injected under ovarian bursa, we detected very few metastases in *Fabp4*$^{-/-}$ mice (4 ± 2 (*Fabp4*$^{-/-}$) versus 181 ± 25 (WT) metastatic nodules; **Fig. 4e**). To directly test the role of FABP4 in the host adipocytes, we cultured ID8 cells with adipocytes from *Fabp4*$^{-/-}$ and WT mice. Lipid content was reduced in ID8 cells cultured with *Fabp4*$^{-/-}$ adipocytes as compared to those cultured with WT adipocytes (**Fig. 4f**). These data identify FABP4 as a key mediator of ovarian cancer cell–adipocyte interactions in the host and potentially in the cancer cells by increasing lipid availability and supporting metastasis (**Fig. 4g**). Therefore, FABP4 emerges as an excellent target in the treament of intra-abdominally disseminating tumors that preferentially metastasize to adipose tissue, such as ovarian, gastric and colon cancers.

In summary, our findings suggest that adipocytes act as major mediators of ovarian cancer metastasis to the omentum. Adipocytes promote the initial homing of tumor cells to the omentum through adipokine secretion. Subsequently, adipocytes provide fatty acids to the cancer cells, fueling rapid tumor growth. This mechanism may not be limited to ovarian

cancer cells and provides a rationale for growth of other malignant cell types that metastasize abdominally or in an adipocyte-rich environment (for example, in breast tissue). This concept is supported by several recent reports that suggest the tumor microenvironment promotes growth of breast cancer cells and provides a rationale for the development of targeted therapies that hinder cancer metabolism fueled by the microenvironment[27,28]. Current research on tumor lipid metabolism focuses primarily on *de novo* fatty acid synthesis in oncogene-transformed tumor cells via glycolysis and glutaminolysis[29,30]. However, our work suggests that tumor lipid metabolism is regulated not only by genetic and epi-genetic changes in the tumor cells but also by the availability of lipids in the microenvironment. Indeed, lipid metabolism and, more specifically, fatty acid metabolism contribute to tumorigenesis[31–34]. Finally, FABP4, a mediator of lipid trafficking in adipocytes and potentially in tumor cells, may provide a therapeutic target to effectively impede intraabdominal metastasis and growth.

ONLINE METHODS

Adipocyte extraction

Adipocytes were extracted from omental, subcutaneous, peritoneal, bowel mesenteric and normal adjacent omental (adjacent to omental tumor, denoted as cancer-associated) tissues. Tissue specimens were obtained from female subjects undergoing surgical procedures for benign conditions or tumor debulking for ovarian cancer treatment at the University of Chicago Medical Center. Informed consent was obtained from each subject before surgery, and the study was approved by the Institutional Review Board at the University of Chicago. Adipose tissue was transported in saline and minced in DMEM/F12 medium containing 0.2% (wt/vol) collagenase type I and 0.1% (wt/vol) BSA. Minced adipose tissue was incubated at 37 °C on a rotary shaker at 80 r.p.m. for 1 h. Undigested tissue was removed after filtration through a 250-μm mesh filter, and mature adipocytes were collected by centrifugation at 200g[5]. There was no contamination from other cell types (**Supplementary Fig. 1a**). Adipocytes were used in experiments by their packed cell volume or counted using a hemocytometer and maintained in DMEM/F12 medium containing 0.1% BSA, denoted as SFM. This method was also used to isolate visceral adipocytes from mice.

In vivo and in vitro homing and adhesion assays

For *in vivo* homing experiments, CMPTX-labeled SKOV3ip1 ovarian cancer cells (4×10^6) were pretreated (30 min) with inhibitory antibodies (R&D Systems) to CXCR1 (MAB330), IL-6R (MAB227) or mouse IgG control (MAB002). Mice were pretreated with 100 μg per kg body weight TIMP-1–specific (R&D Systems AF970) or goat IgG (R&D Systems AB108C) antibodies 30 min before cancer cell injection. Labeled SKOV3ip1 cells were injected intraperitoneally into female athymic nude mice. The omentum was removed 20 min later, digested in 1% (vol/vol) NP-40, and fluorescence was measured using a plate reader. *In vitro* homing was assessed by preparing a Matrigel plug in chamber slides. The plugs consisted of growth-factor–reduced Matrigel and human omental adipocytes in SFM containing an inhibitory antibody or a goat IgG control, in triplicate. Inhibitory antibodies (R&D Systems) to the following proteins were used at the following concentrations: IL-6 (AB206NA) and IL-8 (AB208NA), 50 ng ml^{-1}; MCP-1 (AB279NA), 100 μg ml^{-1}; MMP-9

(EMD Chemicals, IM09L), 6 μg ml^{-1}; TIMP-1, 100 ng ml^{-1}. CMFDA-labeled SKOV3ip1 cells (3×10^6) were added to a culture dish containing the plugs in 6 ml SFM. The plate was then incubated at 37 °C for 30 min. Plugs were removed, and fluorescence was measured using a plate reader. *In vitro* adhesion to equal portions (wt/wt) of full human omentum was carried out in low adhesion plates. Omentum was preincubated in a TIMP-1 inhibitory antibody or a control goat IgG antibody (100 μg ml^{-1}). CMFDA-labeled SKOV3ip1 cells (4×10^6) were pretreated (30 min) with inhibitory antibodies to CXCR1, IL-6R or mouse IgG control. Cancer cells were added to the full omentum (separate wells for each treatment) and allowed to adhere for 20 min at 50 r.p.m. and 37 °C on a rotary shaker. Omentum was then digested in 1% NP-40, and fluorescence was measured using a plate reader.

Fatty acid oxidation

β-oxidation of fatty acids was assessed using a previously described method[35], with minor modifications. Cancer cells were incubated with and without adipocytes (by packed cell volume, 1:3) for 24 h, in triplicate. Adipocytes were washed away, and the medium was changed to Krebs-Ringer's buffer containing 22 μm sodium palmitate, 7.48 μM fatty-acid–free BSA and 5 μCi [9,10(*n*)-^{3}H] palmitic acid per ml and incubated at 37 °C for 0–3 h. Etomoxir (10 μm, Sigma-Aldrich) and L-carnitine (1 mM, Sigma-Aldrich) were added to wells as negative and positive controls, respectively. At the completion of each incubation period, the supernatant from each well was transferred to a microfuge tube containing 5% trichloroacetic acid to stop the reaction. Samples were centrifuged at 16,000*g*, and the supernatant was transferred to a tube containing 1 N sodium hydroxide. Samples were then applied to a column (90 μM, Spectrum Labs) containing 0.5 g ml^{-1} Dowex-1X8 ion-exchange resin and eluted with 1 ml deionized water. ^3H_2O was quantified by scintillation counting. Radioactive ^3H_2O secreted into the medium was normalized to the cellular protein content in each well.

Reverse-phase protein array

Solid tumor nodules from the ovary and the omentum of 22 postmenopausal subjects, macroscopically and microscopically devoid of adipose tissue, were collected at cytoreductive surgery and snap frozen. Clinicopathologic information was collected prospectively[11]. Tissue sections were examined and verified histopathologically to be stage IIIC–IV serous-papillary adenocarcinomas by gynecologic pathologists. Triplicate sets of samples were dissected from the underlying stroma and used for analysis. Tissue samples were homogenized and spotted on nitrocellulose-coated FAST slides (Schleicher & Schuell BioScience) using an Aushon 2470 robotic printer (Aushon Biosystems). Validated primary antibodies were used to probe each slide. The slides were analyzed using Microvigene software (VigeneTech), as previously reported[20,36]. The estimated protein concentrations were normalized by a median polish method and corrected for protein loading using the average expression levels.

Supplementary Material

Refer to Web version on PubMed Central for supplementary material.

Acknowledgments

We thank A.F. Haney (University of Chicago) for collecting omental biopsies and D. Bernlohr (University of Minnesota) for helpful discussions and kindly providing the FABP4 inhibitor. We thank S. Dogan for her contribution to the initiation of this project, G. Isenberg (University of Chicago) for editing the manuscript and A. Mitra (University of Chicago) for helpful discussions regarding the *in vitro* homing assay. We also thank K. Roby (University of Kansas Medical Center), N. Auersperg (University of British Columbia) and C. Clevenger (Northwestern University) for providing the ID8, IOSE and T47D cell lines, respectively. Finally, we thank all the patients, resident physicians and attending physicians in the Department of Obstetrics and Gynecology at the University of Chicago; without their commitment to tissue donation, this project would not have been possible. E.L. holds a Clinical Scientist Award in Translational Research from the Burroughs Wellcome Fund. He is also supported by grants from the Ovarian Cancer Research Fund (Liz Tilberis Scholars Program), the US National Cancer Institute (R01 CA111882) and Bears Care, the charitable beneficiary of the Chicago Bears Football Club. K.M.N. is funded by a Cancer Biology Training Grant from the Committee on Cancer Biology at the University of Chicago and the National Cancer Institute (T32 CA959421). H.A.K. is supported by an award from the National Cancer Institute K99 CA134750). G.S.H. is supported by a grant from the US National Institute of Diabetes and Digestive and Kidney Diseases (R01 DK064360).

References

1. Landen CN, Birrer MJ, Sood AK. Early events in the pathogenesis of epithelial ovarian cancer. J. Clin. Oncol. 2008; 26:995–1005. [PubMed: 18195328]
2. Cho KR, Shih I-M. Ovarian cancer. Annu. Rev. Pathol. 2009; 4:287–313. [PubMed: 18842102]
3. Folkins AK, Jarboe EA, Roh MH, Crum CP. Precursor to pelvic serous carcinoma and their clinical implications. Gynecol. Oncol. 2009; 113:391–396. [PubMed: 19237187]
4. Lengyel E. Ovarian cancer development and metastasis. Am. J. Pathol. 2010; 177:1053–1064. [PubMed: 20651229]
5. Rodbell M. Metabolism of isolated fat cells. J. Biol. Chem. 1964; 239:375–380. [PubMed: 14169133]
6. Merritt WM, et al. Effect of interleukin-8 gene silencing with liposome-encapsulated small interfering RNA on ovarian cancer cell growth. J. Natl. Cancer Inst. 2008; 100:359–372. [PubMed: 18314475]
7. Nilsson MB, Langley RR, Fidler IJ. Interleukin-6 secreted by human ovarian carcinoma cells is a potent proangiogenic cytokine. Cancer Res. 2005; 65:10794–10800. [PubMed: 16322225]
8. Manabe Y, Toda S, Miyazaki K, Sugihara H. Mature adipocytes, but not preadipocytes, promote the growth of breast carcinoma cells in collagen gel matrix culture through cancer-stromal cell interactions. J. Pathol. 2003; 201:221–228. [PubMed: 14517839]
9. Tokuda Y, et al. Prostate cancer cell growth is modulated by adipocyte–cancer cell interaction. BJU Int. 2003; 91:716–720. [PubMed: 12699491]
10. Dirat B, et al. Cancer-associated adipocytes exhibit an activated phenotype and contribute to breast cancer invasion. Cancer Res. 2011; 71:2455–2465. [PubMed: 21459803]
11. Kaur S, et al. β3-integrin expression on tumor cells inhibits tumor progression, reduces metastasis, and is associated with a favorable prognosis in patients with ovarian cancer. Am. J. Pathol. 2009; 175:2184–2196. [PubMed: 19808644]
12. Elliott BE, Tam SP, Dexter D, Chen ZQ. Capacity of adipose tissue to promote growth and metastasis of a murine mammary carcinoma: Effect of estrogen and progesterone. Int. J. Cancer. 1992; 51:416–424. [PubMed: 1317363]
13. Wakil SJ, Abu-Elheiga LA. Fatty acid metabolism: target for metabolic syndrome. J. Lipid Res. 2009; 50:S138–S143. [PubMed: 19047759]
14. Gonzalez-Yanes C, Sanchez-Margalet V. Signalling mechanisms regulating lipolysis. Cell. Signal. 2006; 18:401–408. [PubMed: 16182514]
15. Sengenès C, et al. Involvement of a cGMP pathway in the natriuretic peptide– mediated hormone sensitive lipase phosphorylation in human adipocytes. J. Biol. Chem. 2003; 278:48617–48626. [PubMed: 12970365]

16. Brasaemle DL, Subramanian V, Garcia A, Marcinkiewicz A, Rothenberg A. Perilipin A and the control of triacylglycerol metabolism. Mol. Cell. Biochem. 2009; 326:15–21. [PubMed: 19116774]
17. Gagnon A, et al. Thyroid-stimulating hormose stimulates lipolysis in adipocytes in culture and raises serum free fatty acid levels in vivo. Metabolism. 2010; 59:547–553. [PubMed: 19846175]
18. Wang W, Guan K-L. AMP-activated protein kinase and cancer. Acta Physiol. (Oxf.). 2009; 196:55–63. [PubMed: 19243571]
19. Munday MR, Campbell DG, Carling D, Hardie DG. Identification by amino acid sequencing of three major regulatory phosphorylation sites on rat acetyl-CoA carboxylase. Eur. J. Biochem. 1988; 175:331–338. [PubMed: 2900138]
20. Carey MS, et al. Functional proteomic analysis of advanced serous ovarian cancer using reverse phase protein array: TGF-β pathway signaling indicates response to primary chemotherapy. Clin. Cancer Res. 2010; 16:2852–2860. [PubMed: 20460476]
21. Hotamisligil GS, et al. Uncoupling of obesity from insulin resistance through a targeted mutation in aP2, the adipocyte fatty acid binding protein. Science. 1996; 274:1377–1379. [PubMed: 8910278]
22. Furuhashi M, Hotamisligil GS. Fatty acid binding proteins: Role in metabolic diseases and potential as drug targets. Nat. Rev. Drug Discov. 2008; 7:489–503. [PubMed: 18511927]
23. Scheja L, et al. Altered insulin secretion associated with reduced lipolytic efficiency in aP2−/− mice. Diabetes. 1999; 48:1987–1994. [PubMed: 10512363]
24. Furuhashi M, et al. Treatment of diabetes and atherosclerosis by inhibiting fatty-acid-binding protein aP2. Nature. 2007; 447:959–965. [PubMed: 17554340]
25. Hertzel AV, et al. Identification and characterization of a small molecule inhibitor of fatty acid binding proteins. J. Med. Chem. 2009; 52:6024–6031. [PubMed: 19754198]
26. Uysal KT, Scheja L, Wiesbrock SM, Bonner-Wier S, Hotamisligil GS. Improved glucose and lipid metabolism in genetically obese mice lacking aP2. Endocrinology. 2000; 141:3388–3396. [PubMed: 10965911]
27. Martinez-Outschoorn UE, et al. The autophagic tumor stroma model of cancer or “battery-operated tumor growth” a simple solution to the autophagy paradox. Cell Cycle. 2010; 9:4297–4306. [PubMed: 21051947]
28. Pavlides S, et al. The reverse Warburg effect: aerobic glycolysis in cancer associated fibroblasts and the tumor stroma. Cell Cycle. 2009; 8:3984–4001. [PubMed: 19923890]
29. Levine AJ, Puzio-Kuter AM. The control of the metabolic switch in cancers by oncogenes and tumor suppressor genes. Science. 2010; 330:1340–1344. [PubMed: 21127244]
30. DeBerardinis RJ, Lum JJ, Hatzivassiliou G, Thompson CB. The biology of cancer: Metabolic programming fuels cell growth and proliferation. Cell Metab. 2008; 7:11–20. [PubMed: 18177721]
31. Liu Y. Fatty acid oxidation is a dominant bioenergetic pathway in prostate cancer. Prostate Cancer Prostatic Dis. 2006; 9:230–234. [PubMed: 16683009]
32. Zaugg K, et al. Carnitine palmitoyltransferase 1C promotes cell survival and tumor growth under conditions of metabolic stress. Genes Dev. 2011; 25:1041–1051. [PubMed: 21576264]
33. Pike LS, Smift AL, Croteau NJ, Ferrick DA, Wu M. Inhibition of fatty acid oxidation by etomoxir impairs NADPH production and increases reactive oxygen species resulting in ATP depletion and cell death in human glioblastoma cells. Biochim. Biophys. Acta. 2011; 1807:726–734. [PubMed: 21692241]
34. Hernlund E, et al. Potentiation of chemotherapeutic drugs by energy metabolism inhibitors 2-deoxyglucose and etomoxir. Int. J. Cancer. 2008; 123:476–483. [PubMed: 18452174]
35. Moon A, Rhead WJ. Complementation analysis of fatty acid oxidation disorders. J. Clin. Invest. 1987; 79:59–64. [PubMed: 3793932]
36. Hennessy BT, et al. A technical assessment of the utility of reverse phase protein arrays for the study of the functional proteome in non-microdissected human breast cancers. Clin. Proteomics. 2010; 6:129–151. [PubMed: 21691416]

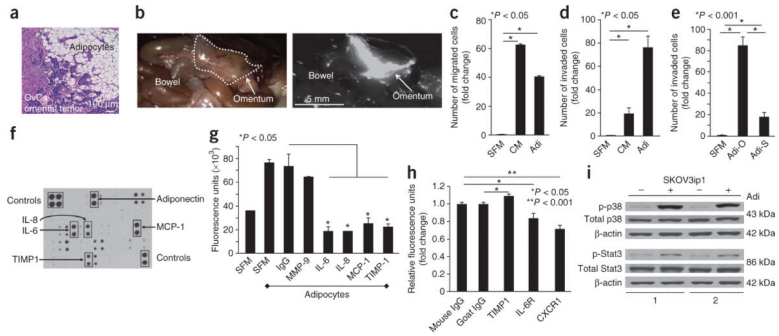

Figure 1.

Adipocytes promote homing of ovarian cancer cells to the omentum. (**a**) H&E staining of ovarian cancer (OvCa) tumor cells invading adipocytes in the human omentum. (**b**) *In vivo* homing assay. Fluorescently-labeled SKOV3ip1 human ovarian cancer cells were injected intraperitoneally into nude mice. Cancer cell localization was detected after 20 min ($n = 6$ mice). The mouse omentum is outlined in the bright-field image (left) and visible in the fluorescent image (right). (**c,d**) Migration (c) and invasion (d) of SKOV3ip1 cells toward serum-free medium (SFM), adipocyte-conditioned medium (CM) and primary human omental adipocytes (Adi). Bars report mean fold change ± s.e.m. One of three experiments, each using a different human subject samples, is shown. (**e**) Invasion of SKOV3ip1 cells comparing primary human omental (Adi-O) and subcutaneous (Adi-S) adipocytes from the same individual. Bars report mean fold change ± s.e.m. One of two experiments shown. (**f**) Cytokine expression in conditioned medium from primary human omental adipocytes. One of four arrays shown. (**g**) Fluorescence intensity of labeled SKOV3ip1 cells that homed to Matrigel plugs containing SFM or adipocytes in the presence or absence of inhibitory antibodies. Bars report means ± s.e.m. One of three experiments shown. (**h**) Fluorescence intensity of labeled SKOV3ip1 cells that adhered to sections of human omentum. SKOV3ip1 cells were pretreated with a CXCR1- or IL-6R–blocking antibody, or whole omentum sections were pretreated with a TIMP-1 inhibitory antibody ($n = 5$ sections per group).Bars report means ± s.e.m. from one of three experiments. (**i**) Immunoblot of total and phosphorylated (p) p38 (Thr180/Tyr182) and Stat3 (Ser727) in SKOV3ip1 cells cultured alone (−) or with (+) adipocytes from two human subject samples for 24 h. One of three experiments shown.

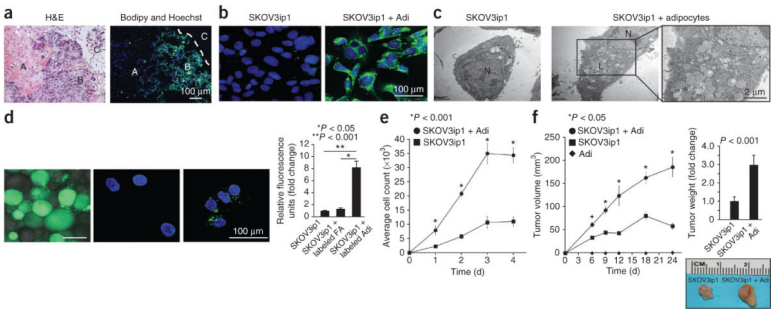

Figure 2.

Ovarian cancer cells use adipocyte-derived lipids for tumor growth. (**a**) Lipid (green) accumulation in human omental metastatic ovarian cancer. The interface between ovarian cancer cells and adipocytes is indicated by a dashed line (H&E staining). Ovarian cancer cells (A) that do not interact with adipocytes (C) lack intracellular lipid staining. The ovarian cancer cells in contact with adipocytes (B) contain more intracellular lipids (nuclear counterstaining, blue). (**b,c**) Lipid (green) accumulation in SKOV3ip1 cells cultured alone or with primary human omental adipocytes (repeated with two additional human subject samples), as determined using confocal microscopy (**b**), or fixed and examined with transmission electron microscopy (**c**) (N, nucleus; L, lipid droplets). (**d**) Fluorsescently labeled fatty acids (FAs) were incubated with and taken up by adipocytes (left) or SKOV3ip1 cells (middle). The labeled adipocytes were cocultured with SKOV3ip1 cells, the adipocytes were removed, and the labeled FAs that were transferred from adipocytes to SKOV3ip1 cells were detected by confocal microscopy (right). Fluorescence quantification is in the right graph. Bars report means ± s.e.m. from one of three experiments, conducted with different human subject samples. (**e**) *In vitro* proliferation of SKOV3ip1 cells alone or cocultured with adipocytes over 4 d. Graph reports means ± s.e.m. from one of three experiments, completed using different human subject samples. (**f**) *In vivo* growth of subcutaneous tumors after injection of SKOV3ip1 cells with or without adipocytes in each flank of the same mouse. Graphs depict tumor volume measured over 24 d (left) and final tumor weight (right). Representative tumor images from one mouse are included (three or four mice per group). Graphs report means ± s.e.m. from one of three experiments, conducted using omental adipocytes from different human subject samples.

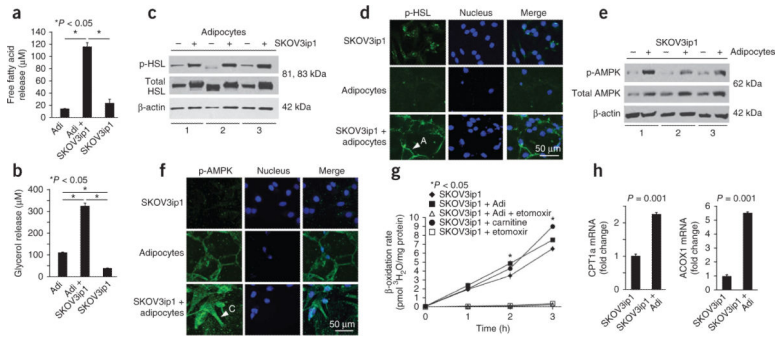

Figure 3.

Cocultivation of ovarian cancer cells with adipocytes activates lipolysis in adipocytes and β-oxidation in cancer cells. (**a,b**) Free fatty acid (**a**) and glycerol release (**b**) are detected in primary human adipocytes cultured alone or with SKOV3ip1 cells alone. Bars report means ± s.e.m. from one of two experiments completed using omental adipocytes from different human subject samples. (**c**) Immunoblot for total and phosphorylated (p) HSL (Ser660) in adipocytes from three different human subject samples cultured with (+) and without (−) SKOV3ip1 cells. (**d**) Immunofluorescence using confocal microscopy for p-HSL (green) in SKOV3ip1 cells, adipocytes or a coculture of both. Arrowhead indicates an adipocyte (A) (nuclear counterstaining, blue). One of two experiments, conducted using different human subject samples, is shown. (**e**) Immunoblot for total and p-AMPK in SKOV3ip1 cells cocultured with (+) and without (−) adipocytes for 24 h from three different human subject samples. (**f**) Immunofluorescence using confocal microscopy for p-AMPK (Thr172, green) in SKOV3ip1 cells, adipocytes, or a coculture of both. Arrow points out a cancer cell (**C**) in the image (nuclear counterstaining, blue). One of two experiments, completed with different human subject samples, is shown. (**g**) β-oxidation rate in SKOV3ip1 cells cocultured with adipocytes (L-carnitine, positive control; etomoxir, negative control). Graph reports means at the indicated times ± s.e.m. One of three experiments, conducted with or without different human subject samples, is shown. (h) mRNA expression of the rate-limiting fatty acid oxidation enzymes carnitine palmitoyltransferase 1 (CPT) and acyl-CoA oxidase 1 (ACOX1) in SKOV3ip1 cells cultured alone or with adipocytes. Bars report mean fold change relative to glyceraldehyde 3-phosphate dehydrogenase expression ± s.e.m. One of three experiments, conducted with different human subject samples, is shown.

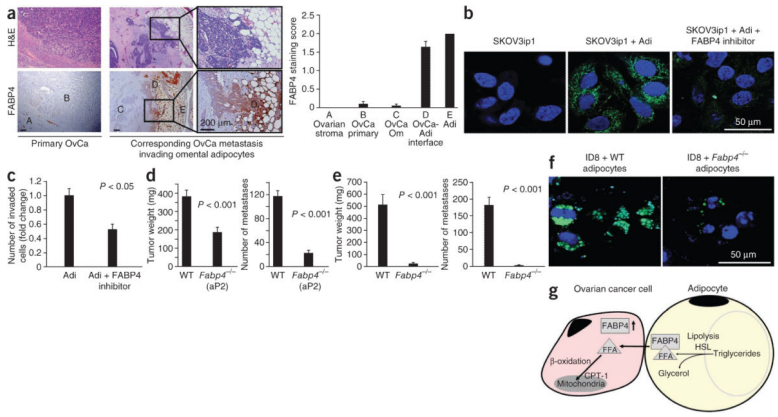

Figure 4.

FABP4 has a key role in the interaction of cancer cells with adipocytes. (**a**) Representative immunohistochemical staining (bottom) for FABP4 in serial sections of primary ovarian tumor and corresponding omental metastatic tissues from a subject with stage IIIC advanced serous ovarian cancer (as classified by the International Federation of Gynecology and Obstetrics). H&E staining is in the top images. The graph on the right is a summary of FABP4 protein expression scoring in 20 subjects, as assessed by immunohistochemistry. The scoring (0, 1 or 2, corresponding to negative, weak or strong) was performed in different tissue compartments: Benign ovarian stroma (A), primary ovarian cancer in the ovary (B), ovarian cancer metastasis to the omentum (C), interface of ovarian cancer cells into adipocytes (Adi) (D) and adipocytes (E). Error bars, ± s.e.m. (**b**) Confocal microscopy images of lipid accumulation (green) in SKOV3ip1 cells cocultured with or without primary human omental adipocytes and a FABP4 inhibitor (nuclear counterstaining, blue). One of two experiments, conducted with different human subject samples, is shown. (**c**) Invasion assay of SKOV3ip1 cells toward adipocytes in the absence or presence of a FABP4 inhibitor. Bars report mean fold change ± s.e.m. One of two experiments, using two different human subject samples, is shown. (**d**) Metastatic tumor burden in *Fabp4*$^{-/-}$ (n = 23) or WT (n = 28) mice 10 weeks after intraperitoneal injection of ID8 mouse ovarian cancer cells (5 × 10^6). Bars report means ± s.e.m. (**e**) Metastatic tumor burden in *Fabp4*$^{-/-}$ (n = 6) or WT (n = 7) mice 90 d after orthotopic injection of ID8 cells under the ovarian bursa. Bars report means ± s.e.m. (**f**) Images generated by confocal microscopy of intracellular lipid accumulation (green) in ID8 cells cocultured with visceral adipocytes extracted from *Fabp4*$^{-/-}$ or WT mouse adipose tissue (nuclear counterstaining, blue). (**g**) Summary of metabolic changes that occur in interacting ovarian cancer cells and adipocytes as described in the text.